Solar Energy Materials & Solar Cells 245 (2022) 111893

Contents lists available at ScienceDirect

Solar Energy Materials and Solar Cells

journal homepage: www.elsevier.com/locate/solmat

Oil-in-Oil emulsions of stearic acid dispersed in silicone oil with enhanced energy storage capability for heat transfer fluids

Clara Delgado-Sánchez *, Pedro Partal, María José Martín-Alfonso, Francisco Javier Navarro

Pro²TecS-Chemical Process and Product Technology Research Centre, Department of Chemical Engineering, ETSI. Campus de "El Carmen", Universidad de Huelva, 21071, Huelva, Spain

ARTICLE INFO

Keywords:
Non-aqueous emulsion
Phase change material (PCM)
Phase change material emulsion (PCME)
Rheology
Stability

ABSTRACT

Non-aqueous phase change emulsions are very unknown and promising multifunctional fluids consisting of phase change materials dispersed in carrier fluids, both being oily phases. The oil-in-oil phase change emulsions allow the possibility of using the same medium for latent heat storage and transport under more extreme pressure and temperature conditions. In this paper, stable emulsions composed of stearic acid with a melting point of 68–71 °C dispersed in silicone oil have been developed. Stearic acid-in-silicone oil emulsion samples with different phase concentrations were evaluated by analysing their thermophysical properties, viscous and viscoelastic behaviour and microstructure. Emulsion properties below the melting point of the phase change material were greatly influenced by the concentration of the disperse phase. Thus, as the temperature lowered, a well-developed three-dimensional network of stearic acid crystalline structures interconnected with each other was formed. Furthermore, emulsion physicochemical and thermal stabilities were examined and proved under several mechanical–thermal cycles, withstanding more than 100 cycles in the calorimeter. The results indicate that stearic acid-in-silicone oil emulsions are an attractive candidate for energy storage applications with a phase change enthalpy in emulsions with the 10 wt% of phase change material of 22.32 J/g.

1. Introduction

Thermal energy storage (TES) systems are widely used worldwide for efficient utilization and conservation of off-peak power, waste heat and intermittent energy sources, cleverly exploiting clean energy resources and decreasing energy consumption [1,2]. An efficient, attractive and innovative method of storing thermal energy storage is latent heat storage. Then, the so-called phase change materials (PCMs) use the latent heat of the phase transition to quickly store and release a large amount of energy during the phase changing process, at a constant temperature [3,4]. Thus, PCMs have recently received considerable attention as they substantially contribute to harvest cheap and clean energy from waste heat sources and solar energy, for direct uses or converting to electricity [5,6]. In addition, they also present the potential for effective heat management in various applications such as building, industry or electronic devices [7]. Furthermore, PCMs can be added to conventional heat transfer fluids (HTFs), obtaining latent functionally thermal fluids that exhibit a higher specific heat storage capacity than conventional HTFs. Therefore, they show promising applications in many fields of renewable energy conversion, production, and storage since they remain in a fluid state throughout the phase change process, allowing for easy pump transportation and circulation in the energy storage systems [8–10].

In general, four broad categories are used to classify the thermal fluids that work with latent heat: (1) ice slurries, i.e., mixtures of ice particles and an aqueous solution; (2) clathrate hydrate slurries (CHSs); (3) microencapsulated PCM slurries (MPCMSs), in which the PCM encapsulated into microcapsules and further dispersed into HTFs; and (4) phase change material emulsions (PCMEs), which are formed by dispersing PCM droplets into the continuous phase, usually water, with the help of the surfactants that reduce the interfacial tension between the two phases [11]. The PCMEs, compared with the others PCM systems, show greater potentials and present several advantages, including a simple preparation process, negligible thermal resistance, good operation stability and low cost, which make them an excellent HTF.

Most of the PCME existing literature used as novel HTFs are manufactured by incorporating PCMs into water with the aid of emulsifiers [12–14]. However, the aim of this work is to develop PCMEs by using two non-aqueous phases for thermal energy storage application, of which, to the best of our knowledge, little work has been done so far. In the literature, there are some studies of non-aqueous emulsions

* Corresponding author.
E-mail address: clara.delgado@diq.uhu.es (C. Delgado-Sánchez).

https://doi.org/10.1016/j.solmat.2022.111893
Received 1 March 2022; Received in revised form 2 June 2022; Accepted 11 July 2022
Available online 17 July 2022

Nomenclature

English Letter

T	temperature (°C)
G′	loss modulus (Pa)
G″	storage modulus (Pa)
n	flow index (−)
Ks	consistency index (Pa s^n)
R^2	coefficient of determination
ST	stearic acid
SO	silicone oil

Abbreviation

TES	thermal energy storage
PCM	phase change material
HTF	heat transfer fluid
CHS	clathrate hydrate slurries
MPCM	microencapsulated PCM slurries
PCME	phase change material emulsion
DSC	differential scanning calorimetry
HLB	hydrophilic-lipophilic balance
SAOS	small-angle light scattering
PLOM	polarized light optical microscope

Greeks

λ	wavelength (nm)
ΔH	enthalpy change (J/g)
η	viscosity (Pa s)
$\dot{\gamma}$	shear rate (s^{-1})

Subscripts

m	melting
c	crystallization

especially for cosmetic and pharmaceutical applications [15,16] and other uses covering crystallization processes within emulsified systems, especially in the food industry [17,18]. However, there is almost no research concerning non-aqueous PCMEs as latent functionally HTFs. Only recently, the authors have begun to study and develop anhydrous PCMEs in previous work [19,20], facing the lack of information regarding the availability of suitable surfactants in such systems and pointing out the difficulty in developing such systems. In that sense, these previous works noted the importance of a good selection of immiscible phases, since a partial compatibility of the phases would mean a loss of their energy storage properties.

These almost totally unknown non-aqueous phase change emulsions would not only present the advantages that slurries bring to heat transfer applications, such as the possibility of using the same medium for transport and storage, the high heat transfer rate due to the increase of the specific surface area of the PCM or the easy of pumping transportation and circulation [9], but also all those related to the use of oily phases, making a difference. Thus, anhydrous PCMEs would allow the transport mass and heat in systems where the pressure and temperature conditions are more extreme [21], those systems could withstand much higher temperature and pressure peaks than current aqueous systems without being degraded. Moreover, they will provide a better long term chemical stability. And, additionally, this study of non-aqueous phase change emulsions will lay the groundwork for the use of PCME in applications with phase change temperatures above 100 °C, offering the advantage of the emulsions to applications where the current water-based dispersions have been restricted due to the upper temperature limit. Therefore, this work can be considered as preliminary work for the next major challenge, the development of emulsions that can be used in high efficient thermal solar collectors (100 °C), industrial heat recovery (<150 °C) [22], and low and intermediate temperature solar collection systems (100-250 °C) [23].

Before going any further, it is worth noting that emulsion cooling below the disperse phase melting point will lead to droplets solidification and, therefore, the formation of a suspension of solid particles. Even though it would be more accurate to call them dispersions (being emulsions above the disperse phase melting point and suspensions below the crystallization temperature), the term phase change material emulsion (PCME) is widely accepted in the literature and will be used throughout this study.

In this work, novel non-aqueous emulsions prepared with stearic acid and silicone oil were explored for developing PCMEs. Stearic acid is a very promising PCM for latent heat storage systems since its variation in both melting temperature and latent during repeated heating/cooling cycles in service is negligible and, therefore, shows a good thermal reliability as PCM [24,25]. Moreover, its phase changing temperature of around 69 °C makes it suitable for applications in the medium temperature range such as solar air heater, solar domestic hot water systems, flat-plate solar collectors, etc. [3,26]. In addition, stearic acid is a safe, cheap, and environmentally friendly PCM fatty acid. On the other hand, silicone oil has been selected as a continuous phase because it is highly stable (chemically and heat resistant) and presents a low viscosity [27].

With this aim, a comprehensive investigation of the thermorheological characteristics of stearic acid-in-silicone oil emulsions stabilized using a silicone surfactant has been carried out. Firstly, the thermophysical properties of the emulsion to secure their applicability for thermal energy storage were evaluated. Secondly, the viscous and viscoelastic behaviour were studied on the basis of the obtained rheological properties and finally, the microstructure was also examined.

2. Materials and methods

2.1. Materials

Non-aqueous stearic acid-in-silicone oil (o/o) phase change emulsions are dispersions of stearic acid droplets in silicone oil stabilized by a selected surfactant. Stearic acid (melting point of 69 °C) was purchased from Sigma-Aldrich (Spain) and a selected industrial silicone oil, ESQUIM FH-100, (polydimethylsiloxane, viscosity 0.1 Pa s at 25 °C) was supplied by Esquim S.A. (Spain). The emulsion was stabilized by a silicone-based non-ionic emulsifier, ABIL Care XL80 (Bis-PEG/PPG-20/5 PEG/PPG-20/5 Dimethicone (and) Methoxy PEG/PPG-25/4 Dimethicone (and) Caprylic/Capric Triglyceride; $HLB_{calculated} = 11$), which was kindly supplied by Evonik Nutrition & Care GmbH (Germany).

2.2. Sample preparation

Non-aqueous dispersions were prepared according to the method detailed elsewhere [19], i.e. mixing all the components of the emulsions by a high shear rotor-stator homogeniser, at 80 °C. The emulsions were prepared at the stearic acid/silicone oil (i.e. disperse/continuous phase) weight ratios of 1/99, 5/95 and 10/90, while keeping the surfactant/-disperse phase weight ratio constant at 1/10. Fig. S2 shows a likely structural formulation of the surfactant and its possible stabilisation mechanism in the present emulsion. It is worth mentioning that such a concentration of surfactant was selected thanks to a pre-study where the lowest possible amount of surfactant to maintain a highly stable system was selected. The minimisation of the amount of surfactant was carried out because there was evidence in several studies with others PCMEs that the surfactant presence can reduce the crystallinity of the dispersed

phase [20,28]. Thus, to reduce this effect, if any, this fixed surfactant/disperse phase ratio was selected for the present emulsions.

Each sample was identified by the initials of each phase (ST or SO) followed by the amount of this phase in the emulsion. For instance, ST10SO90 corresponds to an emulsion prepared as explained above, using 10 g of stearic acid, 90 g of silicone oil and 1 g of surfactant (see Fig. S1 at the supplementary information). As an example of emulsion preparation (sample ST5SO95), 0.5 g of the non-ionic emulsifier was dissolved in 95 g of silicone oil at 80 °C, until ensuring homogeneity. Then, 5 g of stearic acid (pre-conditioned at 80 °C to ensure its liquid state) was incorporated drop by drop and emulsified under high shear conditions (at 20000 rpm) for 10 min using an Ultra-Turrax T25 homogeniser (IKA, Germany).

2.3. Methods

2.3.1. Rheological characterization

Rheological characterization was performed in terms of steady flow viscous tests at constant temperature, viscosity temperature ramps at constant shear rate, and small-amplitude oscillatory shear (SAOS) frequency sweep tests.

Isothermal viscous flow measurements, at 40 and 90 °C, below the crystallization temperature and above the melting point of the dispersed phase respectively, were carried out in a controlled-strain rheometer Ares-G2 (TA Instruments, USA) equipped with a Couette geometry (cup of 30 mm diameter and bob of 27 mm diameter and 42 mm length) on steady rotational shear mode. Tests were performed by progressively applying an increasing stepped shear rate ramp from 0.01 to 1000 s^{-1}. In addition, downwards and upwards temperature ramps were performed by imposing a 1 °C/min gradient from 90 to 40 °C, at the constant shear rate of 1 s^{-1}.

On the other hand, small-amplitude oscillatory shear tests were conducted on phase change emulsions using a controlled-stress Physica MCR 501 rheometer from Anton Paar GmbH (Graz, Austria) and plate-plate geometry (1 mm gap and 50 mm diameter). SAOS tests were carried out between 0.03 and 100 rad s^{-1} at different constant temperatures from 40 °C to 90 °C, at steps of 5–10 °C. The rheological tests were carried out within the linear viscoelastic range, previously identified by performing stress sweeps at 1 Hz.

Finally, rotational rheological measurements were performed in duplicate using Small-Angle Light Scattering (SALS) analysis to determine large fluctuations in density and orientation of the samples as well as the influence of the deformation direction on the behaviour of the disperse phase of the emulsion in the shear field during the phase transition. The Rheo-SALS system was attached to the above-mentioned rheometer, Anton Paar MCR 501, equipped with specially designed glass plate-plate geometry, PP43/GL-HT (gap 0.188 mm). The laser beam (wavelength $\lambda = 658$ nm) illuminated the sample vertically down between crossed polarizers and interacts with the microstructure of the crystallizing sample and gets scattered. The scattered light transmitted through the sample was projected on the screen and photographed using a CCD camera. The scattered light depends on the angle between polarizer and analyser, allowing two types of measurements: polarized (polarizer and analyser parallel) and depolarized (polarizer and analyser perpendicular). In the present study, the measurements were carried out only in the depolarized configuration. These tests were conducted under isothermal and non-isothermal conditions as described above.

In order to ensure accurate rheological results, every sample was measured at least twice.

2.3.2. Optical microscopy

A polarized light optical microscope (PLOM) Olympus BX52 (Japan) with a digital camera Olympus C5050Z (objectives of 10x and 20x) and coupled with an LTS-350 Heating-Freezing Stage controlled by a Linkam TP94, manufactured by Linkam Scientific Instruments (UK) was used to study the morphology of the emulsion and droplet sizes. Optical images of samples were obtained under ordinary and cross-polarized light at different temperatures, ranging from 40 to 90 °C. Samples were carefully poured into a sample holder (76 × 26 mm) and spread under a glass coverslip at 90 °C and then conditioned to the measurement temperatures, to avoid the alteration of the crystalline structures in the sample preparation. The emulsion droplet diameters (d32) were measured using Image J software by taking the average of at least 250 droplets and calculated following the method described by [29].

2.3.3. Differential Scanning Calorimetry (DSC)

Differential Scanning Calorimetry (DSC) tests were obtained by using a Q-250 DSC calorimeter (TA Instruments, USA). Around 5–10 mg of samples were subjected to the following procedure: (a) a first heating scan from room temperature to 120 °C was carried to remove the thermal history of the sample; (b) a cooling ramp, to −80 °C; and (c) a second heating ramp, to the same final temperature used for the first heating scan. The selected conditions were: heating/cooling rates of 10 °C/min and a flow of 50 mL/min N_2 as the purge gas. All thermal events were identified, as well as the enthalpy values and crystallization and melting temperatures of the samples were determined. The temperature at which the PCM starts to melt, was obtained from the point of maximum slope of the leading side of the transition peak and extrapolating the heat flow base line on the same side (T onset); the temperature peak was the point at which the largest deviation of the heat flow signal from the virtual baseline is measured (T peak) and the enthalpy of phase change (ΔH) was calculated as the area under the peak by numerical integration. All the results are the average of three replications of each one of three different batches of the emulsions prepared.

3. Results and discussion

Ideally, a PCME should provide a high density of heat storage accompanied with a suitable fluidity and stability. Thus, in order to optimise the system, emulsion samples with different fractions of the PCM were prepared and studied. Initially, their thermo-physical properties were analysed to verify the latent heat storage capacity, which is a necessary condition to be used in heat storage applications. That is because previous results, for other o/o PCMEs, pointed out that the crystallinity (and, therefore, the phase change enthalpy) could be negatively affected by numerous factors compromising the application [20]. Afterwards, the rheological properties of the systems have been studied in both, steady and oscillatory conditions, as well as its stability. And finally, a more detailed look at the morphology of the emulsions through optical microscopy was carried out.

3.1. Thermo-physical properties

As mentioned above, thermal properties play a vital role in applications of PCMEs. DSC curves of the pure components, stearic acid and silicone oil, and the PCMEs with different mass fractions of stearic acid are illustrated in Fig. 1 and their thermo-physical characteristics including melting point (T_m) and enthalpy of melting (ΔH_m) along with their freezing point (T_c) and enthalpy of freezing (ΔH_c) are summarized in Table 1. For the sake of comparison, both enthalpies were normalised per gram of stearic acid (ST) present in the emulsion.

From the DSC results, it can be settled that the incorporation of stearic acid into silicone oil with the aid of surfactant in the PCMEs has little impact on the phase transition enthalpy of the first (Table 1), which is really positive for heat storage applications. However, when compared to pure stearic acid, a slight decrease in both enthalpies (ΔH_m and ΔH_c) for PCMEs is reported, pointing out that some emulsion components may slightly affect the crystallinity of the sample [19,28]. This effect seems to be intensified with the increase of the concentration of silicone oil, but the small amount of sample used for the DSC test gives rise to relatively high values of phase change enthalpies' standard deviations of all the samples (see Table 1), making it difficult to establish a

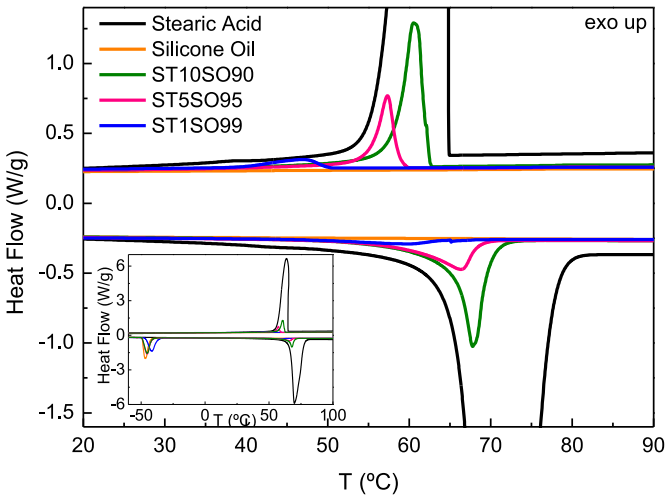

Fig. 1. DSC crystallization and melting curves of the PCMEs with different mass fractions of the stearic acid and the pure components. Inset: more open-ended scale.

clear trend [24,30].

On the other hand, melting and crystallization temperatures clearly decrease with silicone oil content. This observed depression in the melting point and heat of fusion is usually correlated with molecular interactions among the different constituents of the emulsion with the stearic acid that partially disrupts the crystalline structure and, probably, leads to crystallites of smaller sizes. Considering the T onset, which is less affected by heating/cooling rates of the DSC test, it is important to underline that whereas the largest freezing point drop is of about 16 °C, the melting point is modified in a little greater extent specially for the sample ST1SO99 (T_c drops approximately 18 °C). This fact is consistent with the partial compatibility of ST with other molecules inducing a more homogeneous crystallization. As a consequence, the super-cooling degree is almost non-existent for T onset, and rises from 7 to 15 °C for T peak, which is in line with other phase change systems found in literature [31,32]. Therefore, the melting and crystallization events in emulsions seem to be affected by the emulsification process and the concentration of the dispersed phase, particularly at low ST content i.e. emulsion ST1SO99. This effect is probably caused by the high ratio silicone oil/ST resulting much more affected by the processing conditions. This agrees with numerous thermal reliability studies that have been carried out on stearic acid applying repeated working cycles, where similar behaviour where the phase change temperatures and enthalpies decrease slightly has been observed after strong processing [30,33]. Moreover, it is also likely that silicone oil and surfactant form a protective barrier that slows down the crystallization process.

For industrial applications, a PCME must present a suitable thermal stability after a long-term utility period and be able to resist cyclic repeated melting and crystallization cycles. In this sense, a thermal cycling test was conducted to determine the thermal reliability of prepared PCMEs. Fig. 2 portrays DSC curves of ST10SO90 after 100 thermal cycling and shows negligible changes in the melting and crystallization curves after thermal cycling. Therefore, in terms of thermal reliability, stearic acid-in-silicone oil emulsions can be potentially considered for thermal energy storage and transport applications.

Finally, not only in terms of thermal reliability but also in terms of thermal storage capacity the present emulsions show interesting features. Similar values of phase change enthalpy (ΔH_m) of ST10SO90, 21.51 ± 3.6 J/g, have been observed in others aqueous PCMEs. Those PCME with the same application and with analogous PCM (usually paraffins) concentration exhibit very similar values such as 23.3 J/g or 21.1 J/g [28], 19.3 J/g [34], or even lower ones such as 16.5 J/g [35] and 13.9 J/g [8]. Although some of these aqueous emulsions can been prepared with higher PCM concentrations and, therefore, higher phase change enthalpies, the great advantage of the of the here-developed anhydrous PCMEs is the possibility of reaching working temperatures much above the boiling point of water. Moreover, as noted in the introduction, this development may serve as a basis for the development of new non-aqueous PCME with applications in others temperature ranges.

3.2. Rheological measurements

The rheological behaviour of emulsions has become increasingly important for today's formulator in optimising the performance and the attributes of final products [36]. Then, the rheological properties are closely related to their final structure, dispersed phase volume fraction, viscosities of the phases, droplet size or stability of the emulsion [37]. Hence, the rheological characteristics of samples will also have a major influence on the heat transfer process, making it necessary to test the applicability of the PCME systems as HTFs.

3.2.1. Steady-state flow measurements

During in-service operations, stearic acid-in-silicone oil emulsions must be able to recover their rheological properties, after being subjected to a heating-cooling cycle. Therefore, this would give us information on how suitable our material is to be applied as a latent functionally HTF. For this purpose, heating/cooling temperature sweep tests, at a constant shear rate of 1 s^{-1}, were performed to check the

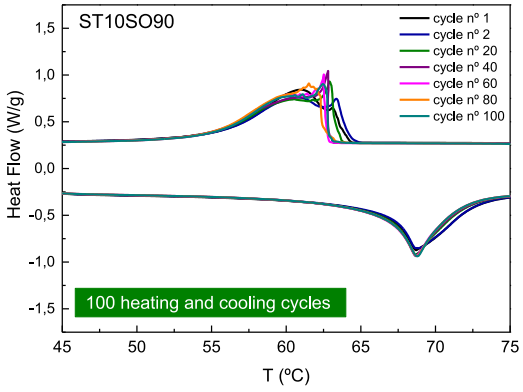

Fig. 2. DSC spectra of ST10SO90 after thermal cycling.

Table 1
Thermo-physical properties of the stearic acid and the PCMEs.

	CRYSTALLIZATION				MELTING			
	T_c onset (°C)	T_c peak (°C)	ΔH_c (J/g)	ΔH_c (J/g of ST)	T_m onset (°C)	T_m peak (°C)	ΔH_m (J/g)	ΔH_m (J/g of ST)
Stearic Acid	64.3 ± 0.8	62.9 ± 0.9	231.74 ± 8.3	231.74 ± 8.3	66.9 ± 0.1	70.9 ± 1.1	229.13 ± 8.3	229.13 ± 8.3
ST10SO90	62.3 ± 0.9	60.6 ± 0.1	22.32 ± 4.4	225.45 ± 44.9	65.4 ± 0.3	67.7 ± 0.4	21.51 ± 3.6	217.22 ± 36.6
ST5SO95	59.1 ± 0.4	57.4 ± 2.2	10.68 ± 0.7	214.65 ± 10.7	59.4 ± 0.5	66.5 ± 0.3	10.38 ± 0.6	208.64 ± 8.0
ST1SO99	48.2 ± 1.6	44.5 ± 2.9	2.2 ± 0.1	220.46 ± 12.3	48.6 ± 2.1	60.1 ± 1.8	1.98 ± 0.1	197.91 ± 10.9

stability of the system. Subsequently, steady state flow curves at different temperatures and linear viscoelastic properties of the resulting emulsions at different temperatures were also evaluated.

In order to study the evolution of the apparent viscosity during the phase change process, Fig. 3 (A) collects the viscosity dependence on temperature of the ST10SO90 system, measured at a shear rate of 1 s^{-1} while subjecting sample to a 1 °C/min cooling/heating ramp. After processing, the sample was cooled from 90 °C to 40 °C at 1 °C/min and then heated from 40 °C to 90 °C at the same rate. As can be seen, during the cooling stage, emulsion viscosity slowly increases until 65 °C where undergone a sharp rise, and thereafter the evolution is slowed down again. This jump in viscosity matches with the onset of the crystallization peak of the dispersed phase observed in DSC scans in Fig. 1. On the other hand, during the subsequent heating cycle, viscosity follows the reverse pathway with the increasing temperature, but with a more abrupt drop at around 65 °C, agreeing with the melting peak of the disperse phase (see again Fig. 1). The small variations between the outward and return paths are consequence of the different mechanisms involved in the melting and crystallization processes that gives rise to the supercooling phenomenon [38]. Additionally, during the heating cycle, an unusual peak in viscosity is observed at around the melting point of stearic acid, followed by a sharp drop to approximately the starting values, which can be related to the melting of the disperse phase and the collapse of its crystalline structure. Regarding the viscosity maximum, this behaviour has been also reported in the literature for similar systems and its origin is a matter of debate [39,40]. However, it seems to be related to a change in the microstructure of the droplets because of the shape relaxation while the subsequent increase of temperature [39,41]. From the operational point of view, a positive fact is that after the cooling and heating cycle, the emulsion is able to retain the previous viscous properties even after being subject to a phase change, point out a suitable rheological stability.

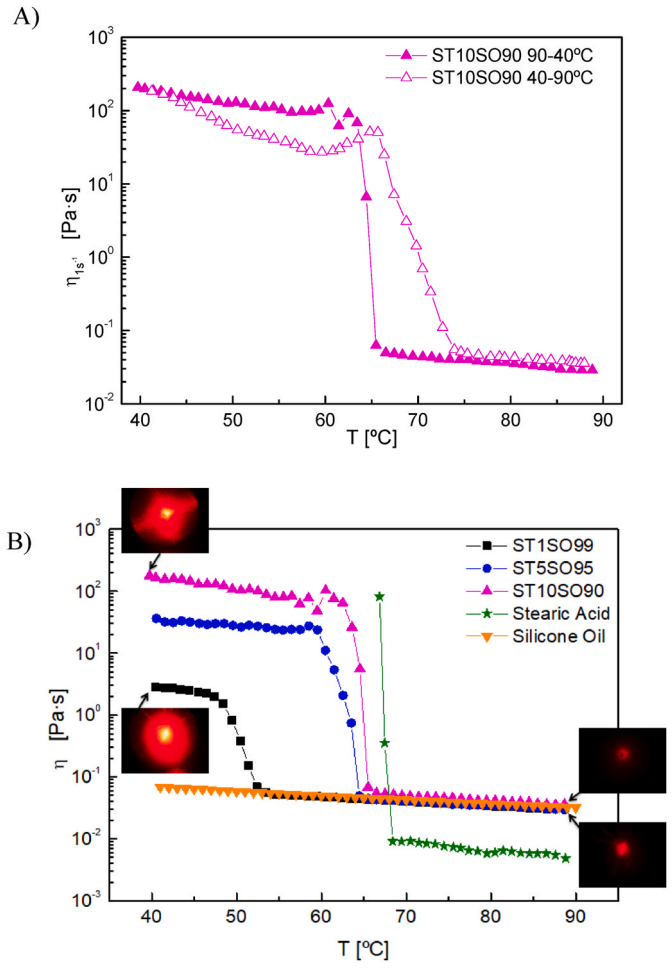

Fig. 3. Temperature dependent viscosity at 1 s^{-1} under 1 °C/min heating/cool ramps conducted on: A) ST10SO90 emulsion (cooling and heating) and B) pure components and stearic acid-in-silicone oil emulsions at different disperse phase concentration (cooling). Inset of SALS crossed-polarizers images.

Fig. 3 (B) shows same testing as above, but only during the cooling ramp, at different disperse phase concentrations. Going deeper in the analysis of their behaviour with decreasing temperature, again, all emulsion viscosities increase rapidly once the phase change process takes place, as the dispersed phase begins to solidify at the freezing temperature. This behaviour is attributed to the formation of solid particles with a much higher viscosity than the liquid droplets and, therefore, less prone to deformation under shear stress [42]. This is in line with the evolution of pristine ST, with a much lower viscosity in molten state and clearly larger values below the freezing point of the solid state (exceeding the instrument limit). In this sense, the apparent viscosity of PCMEs below the freezing point reaches higher values with increasing the dispersed phase concentration. This fact gives clear indication that the development of stearic acid crystals exerts a major role in the rheological behaviour of PCMEs, as has been reported by other authors [28,32]. It is also noteworthy that the steep rise in viscosity occurs at lower temperatures as the concentration of stearic acid decreases, which is fully in line with DSC results of the previous section, where the crystallization temperature decreased accordingly.

In order to more accurately interpret the reported viscosity changes, small-angle light scattering (SALS) analyses were carried out on the emulsions at the extreme temperatures of the range covered (90 and 40 °C). The scattering patterns obtained from the crossed-polarized rheo-SALS analysis are shown as insets in Fig. 3 (B). There were significant differences in the scattering patterns obtained at the start and end of the cooling ramp. Initially, at 90 °C, emulsion displays no scattering with crossed-polarizers configurations (note that central dot is caused by the main beam), as expected for the molten state of any crystallisable structures. However, with decreasing temperature, both an increase in the scattered intensity as well as change in shape to elliptical or four-lobe pattern are observed, which proves the appearance of stearic acid crystals growth during crystallization [43]. A trend to a circularly symmetric pattern means that growing morphologies tend to randomization in space which is expected for the low concentration of crystalline structures (see the inset in ST1SO99 emulsion, Fig. 3 (B)) [44]. Then, the appearance of an indistinct circular pattern may be related to the development of random array of quasi-crystallites smaller than the wavelength of the incident beam [45]. In emulsions with a higher concentration of stearic acid (inset in ST10SO90, Fig. 3 (B)), depolarized SALS image seems to evolve into a four-lobe pattern, a characteristic signature of spherulitic overgrowing morphologies or the existence of rod-like crystalline structures [44,46].

After analysing and confirming that this system can be stable during the phase change process, a more detailed study of the rheological properties of the emulsion before and after the phase change was carried out.

At high temperatures, above the melting point of stearic acid, all emulsions show a Newtonian behaviour with similar viscosity values to the silicone oil, whereas the viscosity of pure stearic acid is significantly lower at 90 °C (Fig. 4 (A)). An increase in the disperse phase concentration does lead to a shorter separation between droplets and a significantly higher specific surface area, both enhancing the interaction between droplets and usually leading to a viscosity raise [47,48]. Thus, it would be expected a higher viscosity with increasing concentration of disperse phase. However, this is not the result found at high temperature. Even though the effect of the droplet size is analysed in detail in the next section, this result seems to be related to the relatively low concentration of the dispersed phase, where the influence of droplet size on the viscosity is of minor importance and the formation of

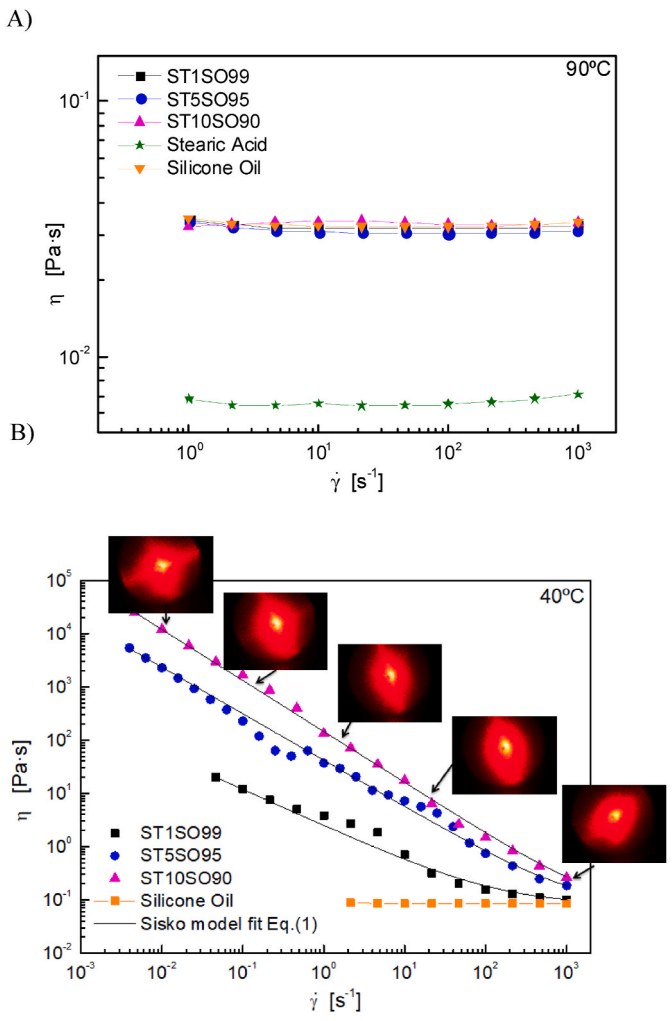

Fig. 4. Viscous flow curves of emulsions and pure components at: A) 90 °C and B) 40 °C, the curves of the emulsions were calculated by Eq. (1). Inset of SALS crossed-polarizers images.

non-flocculated emulsions, as can be clearly seen in Fig. 4 (A) [49].

On the contrary, as can be observed in Fig. 4 (B) at 40 °C, after crystallization, the disperse phase concentration exerts a major influence on the flow curves of dispersions and modifies their rheological behaviour. Then, all samples display a remarkable shear-thinning response, characterised by a drop of up to five orders of magnitude in viscosity and with a trend to reach a limiting viscosity in the high shear rate region.

As a result, the Sisko model fits fairly well the flow behaviour obtained over the whole shear rate range studied ($R^2 > 0.99$) and is useful for analysing this tendency:

$$\eta = \eta_\infty + K_s\,\dot{\gamma}^{n-1} \tag{1}$$

where K_s and n are the consistency and flow indexes, respectively, and η_∞ is the high-shear-rate limiting viscosity. These fitting parameters are shown in Table 2. The decrease in flow index (and $n < 1$) with increasing disperse phase concentration reflects a more apparent shear-thinning behaviour. Even though this result could be partially attributed to the viscosity increase of the stearic acid droplets after their solidification during phase change, the magnitude of the modification in the flow behaviour is not consistent with these moderately diluted non-flocculated dispersions. Therefore, this result hints structural changes in the emulsion microstructure related to the crystallization of the steric acid, apart from the solidification of the dispersed phase.

Table 2
Values of Sisko's model parameters.

Sisko's model parameters				
	η_∞ (Pa s)	Ks (Pa s^n)	n (–)	R^2
ST10SO90	*0.078*	*145.00*	*0.04*	*0.999*
ST5SO95	*0.085*	*41.81*	*0.12*	*0.998*
ST1SO99	*0.080*	*2.43*	*0.31*	*0.990*

As deduced from Fig. 4 (B), a notable increase in viscosity values is noticed as concentration rises, which is in line with the previously reported apparent viscosities in the low-temperature zone of the temperature sweeps shown in Fig. 3 (B) and *Ks* evolution gathered in Table 2. Moreover, parameters recorded in Table 2 reveal that larger disperse phase concentrations lead to a more complex microstructure with stronger inter-droplet interactions that provoke an increase in the flow resistance and, therefore, in the consistency index, K_s [31].

On the other hand, all systems present an interesting trend to reach a similar high-shear-rate limiting viscosity, close to that of the oil forming the continuous phase (see η_∞ values in Table 2). This reveals that dispersion microstructure is highly susceptible to shear, which is clearly positive from the application standpoint because, commonly, industrial processing and pumping operations involve shear rates within the intermediate-high shear regime (1-1000 s^{-1}) [50]. More specifically, shear rates of 1 s^{-1} are typical shear rates of fluid drainage [51], the range 10–10000 s^{-1} are typical shear rates for mixing and stirring, and 100 –1000 s^{-1} for pipe flow [52]. As an example, it can be mentioned that lubricant greases with a marked shear thinning behaviour and having much higher low-shear apparent viscosities (approximately 10^7 Pa s) can be successfully pumped in piping flow experiments [53].

Finally, the SALS images (inset Fig. 4 (B)) also give us information about the effect of applied shear in rotational measurements under isothermal conditions. Preferential orientation of scatters along the flow direction is the consequence of elongated crystalline structures (threads) [44,54]. Differences, as in the case of static measurements shown in the inset of Fig. 3 (B), result from the stronger impact of the applied deformation and the significant effect of the increase in deformation on the pre-formed structure. As crystalline structures are supposed to be rigid and confined into the disperse phase, this behaviour is consistent with their orientation close to the shear direction. Then, this pattern in the polarized rheo-SALS set-up suggests that there is a continuous structure in the flow direction [46]. Then, whereas liquid PCM particles are spherical, after crystallization, solid and distorted particles are expected to appear. The distorted shape results in a higher surface area of the particles that may strengthen the interaction forces. Therefore, such an interrelated microstructure would largely affect the flow behaviour and becomes stronger as PCM content increases [55]. Consequently, at low shear rates it leads to a notable viscosity increase and, as shear rate rises, the progressive orientation of the structures gives rise to the viscosity fall. This behaviour is very common for emulsions of phase-shifting materials and has been previously reported [14,28,56].

Dynamic viscoelastic moduli within the linear viscoelastic region provide a fingerprint of the viscoelastic system under non-destructive conditions and give structural information in a regime where excitation does not disturb the equilibrium microstructure of the sample. Thus, the system rheology is examined without disrupting its structure as continuous shear techniques (i.e. viscous flow tests) do.

Oscillatory frequency sweep tests were conducted to obtain information about the developed microstructure after crystallization. The response of the dynamic measurements, the storage (or elastic) modulus G' and the loss (or viscous) modulus G'' are shown in Fig. 5. Each system was also investigated at different temperatures within the application temperature range, since temperature had an important effect on viscoelastic properties, especially when a phase change material is involved.

At low temperature, frequency sweep curves show that the elastic

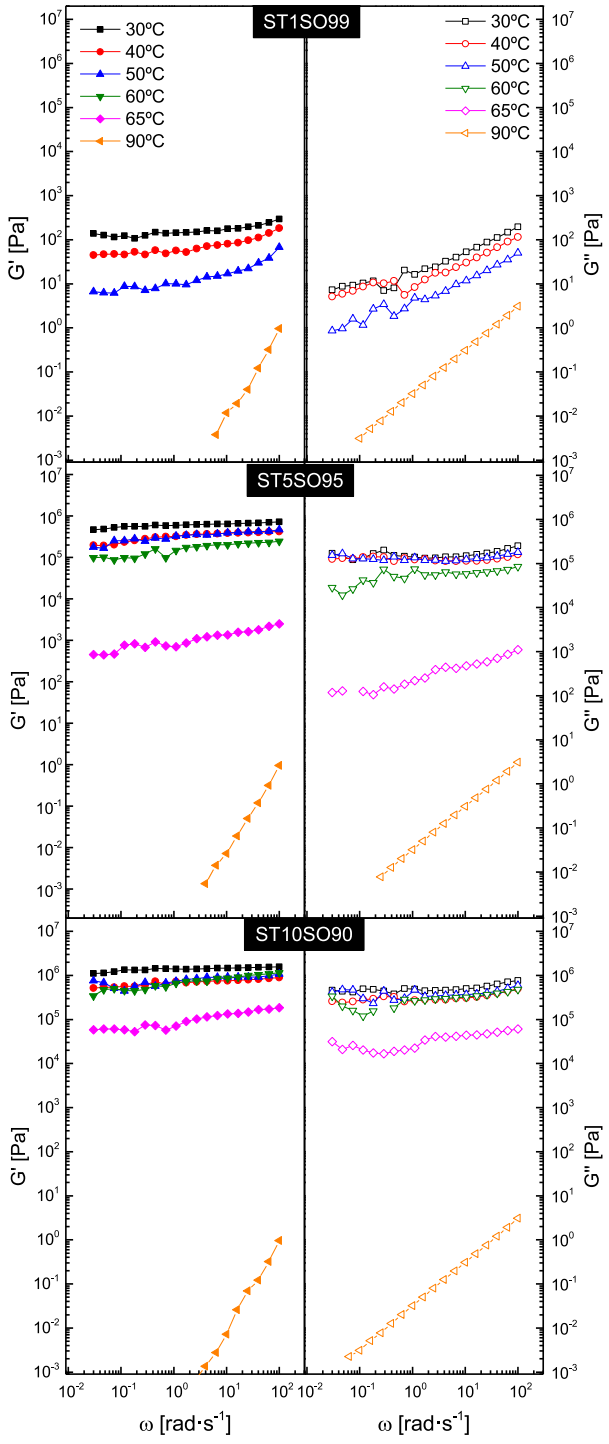

Fig. 5. Storage (*left-hand column*) and Loss (*right-hand column*) moduli as a function of frequency of the emulsions: A) ST1SO99, B) ST5SO95 and C) ST10SO90, at different temperatures.

modulus is almost independent of frequency and remains clearly above the loss modulus (Fig. 5), which develops (or tends to develop) a minimum that depends on the testing temperature and concentration. Therefore, the so-called "plateau region" is noticed pointing out the formation of a gel-like structure when the disperse phase remains in its solid crystalline state [57].

From Fig. 5, it is obvious that the liner viscoelastic behaviour of dispersions strongly depends on the disperse phase concentration, especially when ST content increases from 1 to 5 wt%. Thus, ST1SO99 presents lower G′ and G″ values and a crossover between both linear viscoelastic functions at high frequencies, and exhibits a less evident plateau region. Higher disperse phase concentrations (samples ST5SO95 and ST10SO90) induce a more developed plateau region and a remarkable rise of four orders of magnitude in both moduli. Then, larger dispersed phase concentration favours the formation of stronger gel-like characteristics [58]. Thus, as the volume fraction of the disperse phase increases, the number of stearic acid crystals grows, decreasing the distance between the droplets and increasing the total area of the interface [39,59].

In general, below the melting point of the stearic acid, as temperature increases, both G' and G'' undergo a progressive lowering, while maintaining their rheological behaviour (Fig. 5). At temperatures close to the phase change, the plateau region becomes less evident, and then, a weaker gel is formed as temperature increases.

The reported rheological behaviour that emerges at temperatures around and below the dispersed phase change may be related to the formation of well-developed three-dimensional network as a consequence of the crystallization of the disperse phase. Thus, the formed crystalline structures are probably interconnected with each other, enhancing the network rigidity as temperature lowers [60]. In addition, taking into account that in the molten state a non-flocculated dispersion of spherical droplets is obtained and the disperse phase concentration is relatedly low (Fig. 5), the solidification of the PCM may be accompanied by other processes that significantly change the microstructure of the sample. According to this, such viscoelastic behaviour is consistent with a microstructure where stearic acid forms a crystalline network expanded through the whole volume, swollen by the silicone oil. Thus, the solid-like stearic acid deformable network would contribute to the enhancement of elastic and viscous properties.

As shown in Fig. 5, before the phase change, when the temperature raises, both moduli decrease very slightly in all samples, in line of the previously reported evolution of the apparent viscosity with temperature (Fig. 3).

It is worth mentioning that, unexpectedly ST10SO90 seems to show a minor increase of the viscoelastic functions at 60 °C (Fig. 5 (C)) which approximately corresponds the onset of the melting process in Fig. 1. This is consistent with the local viscosity maximum observed in the temperature sweeps portrayed in Fig. 3, which is more intense as disperse phase concentration increases. This outcome is probably caused by the consolidation of the network structure of the crystalline structures due to the onset of a phase change. The liquefaction of the dispersed phase initially leads to a shape relaxation process and, at concentrations high enough, to the jamming of the dispersed structures due to their expansion giving rise to a change in the network. Similar behaviour was observed in other systems where a phase change of one of the system components takes place [39,40].

At temperatures close to melting point disclosed in Table 1 (50 °C for ST1SO99 and 65 °C for ST5SO95 and ST10SO90) the drop of viscoelastic moduli become more apparent and slopes of these functions increases, but G' still remains over G'' (for ST1SO99 a crossover appears at high frequencies) pointing out a small network weakening. In all systems, the gel collapses sharply at higher temperatures (e.g., 90 °C), with a sudden drop of G′ and G''. Thus, a fluid-like behaviour or the terminal region of the mechanical spectrum is observed, where G''>G′ and both moduli exhibit a power-law dependence on frequency with log-log slopes of 1 and 2, respectively. Finally, it is worth noting that the transition temperature from gel-like to liquid-like response lowers as concentration does, particularly for ST1SO99, in line with the viscosity evolution during cooling reported in Fig. 3 (B).

3.3. Microstructure

As already mentioned, the macro-properties of the samples are closely related to their micro-morphologies [61]. Thus, optical images of samples were obtained at two different temperatures (before and after

the melting point of the PCM, Fig. 6 row (1) and Fig. 6 row (2), respectively) at different disperse phase concentrations (see the columns of Fig. 6). Fig. 6 also gathers images of the emulsions at 40 °C with cross-polarized light to identify the presence of crystalline structures and their distribution throughout the sample (Fig. 6 row (3)).

At 90 °C, above their melting point, where both phases are low-viscosity liquids, optical microscope clearly shows a fairly homogeneous distribution of isolated stearic acid droplets, dispersed in a silicone oil continuous medium (Fig. 6 (A1), (B1) and (C1)). Therefore, at high temperature, when the disperse phase is melted, all emulsions present a non-flocculated microstructure, a fact that would explain their Newtonian flow behaviour.

From these micrographs, the calculated diameters of the droplets slightly increase with the dispersed phase fraction, (3.41 μm in ST1SO99, 4.19 μm in ST5SO95 and 6.58 μm in ST10SO90). According to those results, mean particle size increase with disperse phase concentration. However, their contribution to the bulk viscosity is not high enough to modify the emulsion flow behaviour, due to the relatively low concentration or volume fraction of the disperse phase. Therefore, at 90 °C, the viscosity of the emulsions becomes close to the continuous phase viscosity (Fig. 4 (A)).

On the other hand, during cooling, the microstructure of the emulsion is greatly modified evolving from a non-flocculated state to a more complex arrangement (see Fig. 6 row (2)). Thus, self-assembled structures clearly appear when the temperature of the sample decreases to 40 °C, as a consequence of the crystallization of the disperse phase, as can be seen by inspecting the same samples under cross-polarized light in Fig. 6 row (3), where the light areas correspond to crystals of stearic acid [62]. The crystal microstructure exhibited various morphologies depending on disperse phase concentration. These crystals may protrude from the freezing droplets inducing self-shaping depending on crystal morphology [63], and can be ranged from thin crystallised layer to larger droplets that crystallise in a globular form. Higher concentrations of stearic acid in the emulsion tended to large rod-like structures. As an example, ST5SO95 allows us to analyse the development of the new microstructures, since a three-dimensional crystalline network can be observed together with small globules of crystallised particles (Fig. 7). This can also be seen more clearly in Fig. 8 with lower magnifications. There are many studies currently discussing about the different crystallization mechanisms of droplets in emulsions [64,65]. It has even been shown that the polydispersity of the emulsion affects the rate of crystallization and, therefore, any structure that may form [66]. The latter, together with the different droplet sizes and quantities, explains

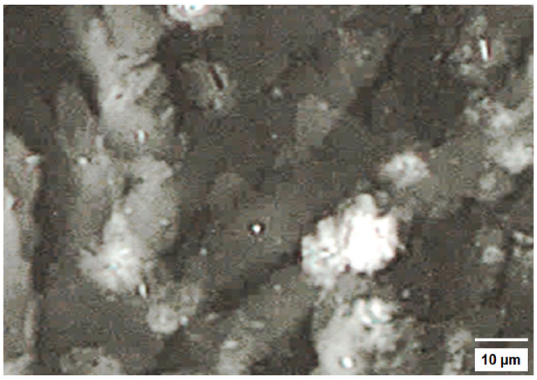

Fig. 7. Detail of the micromorphology under cross-polarized light of ST5SO95.

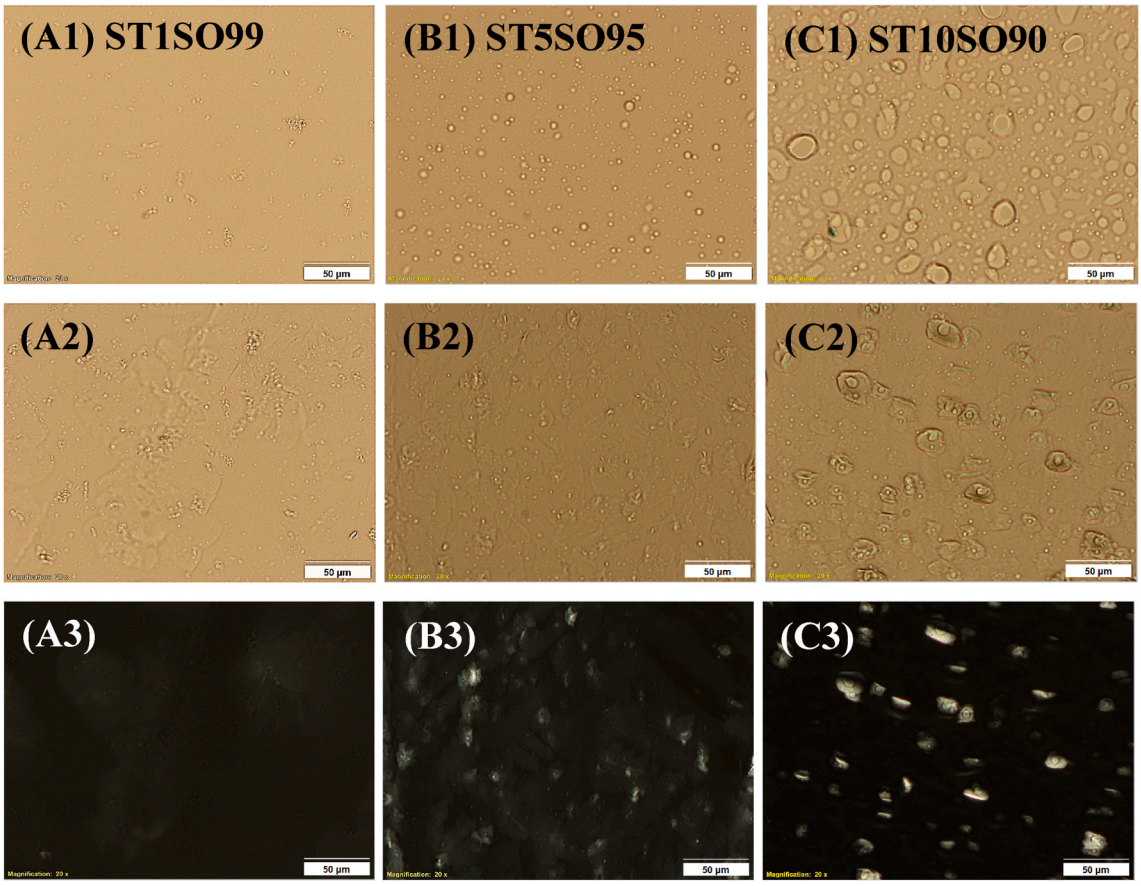

Fig. 6. Micromorphology of the phase change emulsion at different concentrations: column (A) ST1SO99, column (B) ST5SO95, column (C) ST10SO90; under an optical microscope (20x): row (1) at 90 °C; row (2) at 40 °C; row (3) at 40 °C under crossed-polarized light.

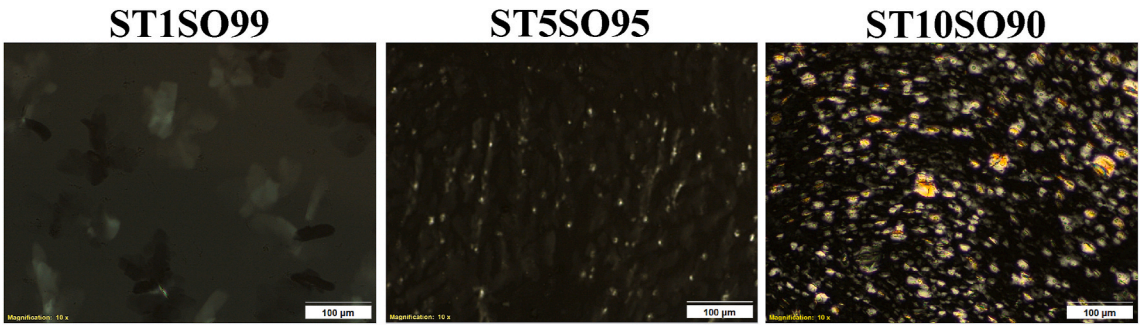

Fig. 8. Micromorphology under cross-polarized light of the phase change emulsion at different concentrations under an optical microscope (10x).

why different structures are observed in emulsions with different dispersed phase concentrations.

What is clear is that non-spherical shapes are triggered by the crystal formation into the droplets upon emulsion cooling. As was assumed in the previous section, emulsion droplets deviated from the initial spherical shape, resulting in a higher surface area of the particles, strengthening the interaction force, which is very common in crystallised systems [32,42]. It has also been observed that crystals protruded from the droplet interface and a three-dimensional network are formed developing an extended microstructure in the system. Therefore, this complex crystal deformable microstructure with strong inter-droplet interactions is consistent with the above results and would explain the reported rheological properties.

Finally, the emulsions microstructure at high temperature has been also evaluated after experiencing 10 heating-cooling cycles. According to the micrographs shown in Fig. 9, PCMEs only showed a slight increase in droplet size after thermal cycling (4.189 µm in ST1SO99, 4.785 µm in ST5SO95 and 6.922 µm in ST10SO90). This result points out that the stearic acid-in-silicone oil emulsions exhibit good thermal stability and is reliable with the results obtained in the previous analyses. Thus, even though droplets are broken by PCM crystals during the cooling cycle, initial microstructure of the emulsion is recovered when reheated up to 90 °C, revealing the high effectiveness of the surfactant.

4. Conclusions

At present, formulating a non-aqueous PCME for thermal storage and heat transfer applications is both promising and challenging. This study assesses in detail the thermal and rheological performance of stearic acid-in-silicone oil emulsions as well as their microstructural and viscoelastic properties at different temperatures. The obtained results make evident that a stable PCME can be successfully fabricated by selecting an appropriate silicone surfactant.

Emulsions were characterised by a Newtonian behaviour at high temperature, above the melting point of the PCM, and a pronounced non-Newtonian shear thinning behaviour, described quantitatively by the Sisko model, at temperature below the melting point of the PCM. After crystallization, the results show an increase in low-shear-rate viscosity of up to 5 orders of magnitude for the most concentrated emulsion. This increase was due to the occurrence of an interrelated microstructure of crystals which would largely affect the flow behaviour of the emulsion and becomes stronger as PCM content increases. Indeed, structural information obtained by non-destructive essays shows as a well-developed three-dimensional network of crystalline structures interconnected with each other was formed as a consequence of the crystallization of the dispersed phase. Interestingly, such a microstructure is highly susceptible to shear, which is clearly positive from the application standpoint, as industrial processing and pumping operations usually involve shear rates within the intermediate-high shear regime.

On the other hand, samples were subjected to heating/cooling temperature sweep tests under steady shear, optical microscopy and DSC, checking not only the rheological and microstructural stability of the system but also its thermal reliability during in-service operations. The present PCMEs were able to resist heating-cooling cycles and remain stable for at least one month, keeping their properties and heat storage capacity practically intact. Consequently, the PCMEs show great potential for use as a novel HTF in thermal energy storage systems. A more in-depth study about the energy transport characteristics and the evaluation of the performance in a pilot plat device, close to the industrial applications, will be the path to continue this study.

CRediT authorship contribution statement

Clara Delgado-Sánchez: Writing – review & editing, Writing – original draft, Resources, Methodology, Investigation, Formal analysis, Data curation, Conceptualization. **Pedro Partal:** Writing – review & editing, Visualization, Validation, Supervision, Project administration, Funding acquisition, Conceptualization. **María José Martín-Alfonso:** Writing – original draft, Resources, Investigation, Formal analysis, Data curation, Conceptualization. **Francisco Javier Navarro:** Writing – review & editing, Visualization, Validation, Supervision, Resources, Project administration, Funding acquisition, Conceptualization.

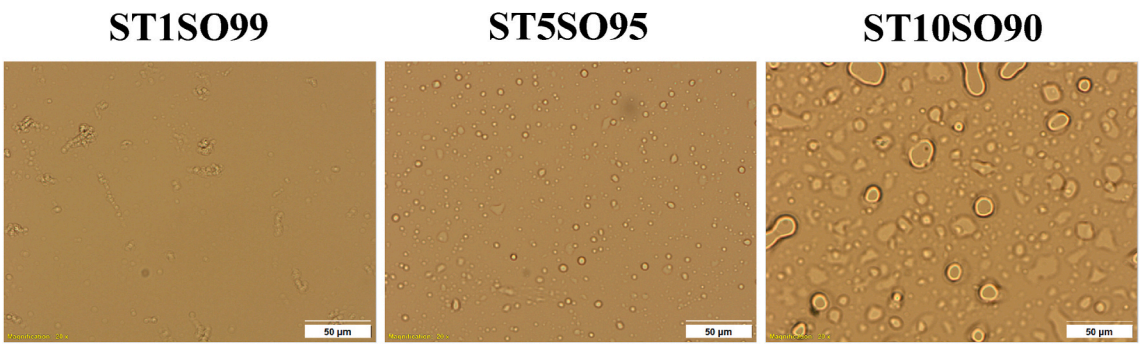

Fig. 9. Micrographs of stearic acid-in-silicone oil emulsions at 90 °C after heating-cooling cycles.

Declaration of competing interest

The authors declare that they have no known competing financial interests or personal relationships that could have appeared to influence the work reported in this paper.

Data availability

Data will be made available on request.

Acknowledgements

Grant PID2020-116905RB-I00 funded by MCIN/AEI/10.13039/501100011033, grant P18-RT-4684 funded by EU-FEDER program and grant CTQ2017-89792-R funded by MCIN/AEI/10.13039/501100011033 and by "ERDF A way of making Europe", by the "European Union".

Appendix A. Supplementary data

Supplementary data to this article can be found online at https://doi.org/10.1016/j.solmat.2022.111893.

References

[1] L.F. Cabeza, Components. Thermal energy storage, in: Ref. Module Earth Syst. Environ. Sci., Elsevier, 2021, https://doi.org/10.1016/B978-0-12-819727-1.00033-9.
[2] L.F. Cabeza, A. de Gracia, G. Zsembinszki, E. Borri, Perspectives on thermal energy storage research, Energy 231 (2021), 120943, https://doi.org/10.1016/j.energy.2021.120943.
[3] K. Du, J. Calautit, Z. Wang, Y. Wu, H. Liu, A review of the applications of phase change materials in cooling, heating and power generation in different temperature ranges, Appl. Energy 220 (2018) 242–273, https://doi.org/10.1016/j.apenergy.2018.03.005.
[4] Z. Khan, Z. Khan, A. Ghafoor, A review of performance enhancement of PCM based latent heat storage system within the context of materials, thermal stability and compatibility, Energy Convers. Manag. 115 (2016) 132–158, https://doi.org/10.1016/j.enconman.2016.02.045.
[5] M. Kenisarin, K. Mahkamov, Solar energy storage using phase change materials, Renew. Sustain. Energy Rev. 11 (2007) 1913–1965, https://doi.org/10.1016/j.rser.2006.05.005.
[6] M.K.A. Sharif, A.A. Al-Abidi, S. Mat, K. Sopian, M.H. Ruslan, M.Y. Sulaiman, M.A. M. Rosli, Review of the application of phase change material for heating and domestic hot water systems, Renew. Sustain. Energy Rev. 42 (2015) 557–568, https://doi.org/10.1016/j.rser.2014.09.034.
[7] Z. Ling, Z. Zhang, G. Shi, X. Fang, L. Wang, X. Gao, Y. Fang, T. Xu, S. Wang, X. Liu, Review on thermal management systems using phase change materials for electronic components, Li-ion batteries and photovoltaic modules, Renew. Sustain. Energy Rev. 31 (2014) 427–438, https://doi.org/10.1016/j.rser.2013.12.017.
[8] P. Sivasamy, A. Devaraju, S. Harikrishnan, Review on heat transfer enhancement of phase change materials (PCMs), Mater. Today Proc. 5 (2018) 14423–14431, https://doi.org/10.1016/j.matpr.2018.03.028.
[9] Z. Youssef, A. Delahaye, L. Huang, F. Trinquet, L. Fournaison, C. Pollerberg, C. Doetsch, State of the art on phase change material slurries, Energy Convers. Manag. 65 (2013) 120–132, https://doi.org/10.1016/j.enconman.2012.07.004.
[10] X. Zhang, J. Niu, J.-Y. Wu, Development and characterization of novel and stable silicon nanoparticles-embedded PCM-in-water emulsions for thermal energy storage, Appl. Energy 238 (2019) 1407–1416, https://doi.org/10.1016/j.apenergy.2019.01.159.
[11] F. Wang, W. Lin, Z. Ling, X. Fang, A comprehensive review on phase change material emulsions: fabrication, characteristics, and heat transfer performance, Sol. Energy Mater. Sol. Cells 191 (2019) 218–234, https://doi.org/10.1016/j.solmat.2018.11.016.
[12] L. Huang, C. Doetsch, C. Pollerberg, Low temperature paraffin phase change emulsions, Int. J. Refrig. 33 (2010) 1583–1589, https://doi.org/10.1016/j.ijrefrig.2010.05.016.
[13] L. Huang, M. Petermann, C. Doetsch, Evaluation of paraffin/water emulsion as a phase change slurry for cooling applications, Energy 34 (2009) 1145–1155, https://doi.org/10.1016/j.energy.2009.03.016.
[14] T. Morimoto, K. Togashi, H. Kumano, H. Hong, Thermophysical properties of phase change emulsions prepared by D-phase emulsification, Energy Convers. Manag. 122 (2016) 215–222, https://doi.org/10.1016/j.enconman.2016.05.065.
[15] A.K.F. Dyab, L.A. Mohamed, F. Taha, Non-aqueous olive oil-in-glycerin (o/o) Pickering emulsions: preparation, characterization and in vitro aspirin release, J. Dispersion Sci. Technol. 39 (2018) 890–900, https://doi.org/10.1080/01932691.2017.1406368.
[16] V. Jaitely, T. Sakthivel, G. Magee, A.T. Florence, Formulation of oil in oil emulsions: potential drug reservoirs for slow release, J. Drug Deliv. Sci. Technol. 14 (2004) 113–117, https://doi.org/10.1016/S1773-2247(04)50022-9.
[17] B.M. Degner, K.M. Olson, D. Rose, V. Schlegel, R. Hutkins, D.J. McClements, Influence of freezing rate variation on the microstructure and physicochemical properties of food emulsions, J. Food Eng. 119 (2013) 244–253, https://doi.org/10.1016/j.jfoodeng.2013.05.034.
[18] F.R. Lupi, D. Gabriele, B. de Cindio, M.C. Sánchez, C. Gallegos, A rheological analysis of structured water-in-olive oil emulsions, J. Food Eng. 107 (2011) 296–303, https://doi.org/10.1016/j.jfoodeng.2011.07.013.
[19] C. Delgado-Sánchez, A.A. Cuadri, F.J. Navarro, P. Partal, Formulation and processing of novel non-aqueous polyethylene glycol-in-silicone oil (o/o) phase change emulsions, Sol. Energy Mater. Sol. Cells 221 (2021), 110898, https://doi.org/10.1016/j.solmat.2020.110898.
[20] C. Delgado-Sánchez, P. Partal, M.J. Martín-Alfonso, F.J. Navarro, Role of crystallinity on the thermal and viscous behaviour of polyethylene glycol-in-silicone oil (o/o) phase change emulsions, J. Ind. Eng. Chem. 103 (2021) 348–357, https://doi.org/10.1016/j.jiec.2021.08.003.
[21] M.M. Kenisarin, High-temperature phase change materials for thermal energy storage, Renew. Sustain. Energy Rev. 14 (2010) 955–970, https://doi.org/10.1016/j.rser.2009.11.011.
[22] V. Soni, A. Kumar, V.K. Jain, Performance evaluation of nano-enhanced phase change materials during discharge stage in waste heat recovery, Renew. Energy 127 (2018) 587–601, https://doi.org/10.1016/j.renene.2018.05.009.
[23] R.Z. Wang, X.Q. Zhai, Development of solar thermal technologies in China, Energy 35 (2010) 4407–4416, https://doi.org/10.1016/j.energy.2009.04.005.
[24] V.N. Chaudhari, M.K. Rathod, K.A. Chaudhari, Stearic acid as phase change material: thermal reliability test and compatibility with some construction materials, Int. J. Eng. Res. Technol. 2 (2013).
[25] H. Masoumi, R. Haghighi khoshkhoo, S.M. Mirfendereski, Modification of physical and thermal characteristics of stearic acid as a phase change materials using TiO2-nanoparticles, Thermochim. Acta 675 (2019) 9–17, https://doi.org/10.1016/j.tca.2019.02.015.
[26] R. Wen, W. Zhang, Z. Lv, Z. Huang, W. Gao, A novel composite Phase change material of Stearic Acid/Carbonized sunflower straw for thermal energy storage, Mater. Lett. 215 (2018) 42–45, https://doi.org/10.1016/j.matlet.2017.12.008.
[27] P. Somasundaran, S.C. Mehta, P. Purohit, Silicone emulsions, Adv. Colloid Interface Sci. 128–130 (2006) 103–109, https://doi.org/10.1016/j.cis.2006.11.023.
[28] J. Chen, P. Zhang, Preparation and characterization of nano-sized phase change emulsions as thermal energy storage and transport media, Appl. Energy 190 (2017) 868–879, https://doi.org/10.1016/j.apenergy.2017.01.012.
[29] A. Timgren, M. Rayner, P. Dejmek, D. Marku, M. Sjöö, Emulsion stabilizing capacity of intact starch granules modified by heat treatment or octenyl succinic anhydride, Food Sci. Nutr. 1 (2013) 157–171, https://doi.org/10.1002/fsn3.17.
[30] A. Sarı, Thermal reliability test of some fatty acids as PCMs used for solar thermal latent heat storage applications, Energy Convers. Manag. 44 (2003) 2277–2287, https://doi.org/10.1016/S0196-8904(02)00251-0.
[31] F. Wang, X. Fang, Z. Zhang, Preparation of phase change material emulsions with good stability and little supercooling by using a mixed polymeric emulsifier for thermal energy storage, Sol. Energy Mater. Sol. Cells 176 (2018) 381–390, https://doi.org/10.1016/j.solmat.2017.10.025.
[32] X. Zhang, J. Wu, J. Niu, PCM-in-water emulsion for solar thermal applications: the effects of emulsifiers and emulsification conditions on thermal performance, stability and rheology characteristics, Sol. Energy Mater. Sol. Cells 147 (2016) 211–224, https://doi.org/10.1016/j.solmat.2015.12.022.
[33] A. Sarı, A. Biçer, Ö. Lafçı, M. Ceylan, Galactitol hexa stearate and galactitol hexa palmitate as novel solid–liquid phase change materials for thermal energy storage, Sol. Energy 85 (2011) 2061–2071, https://doi.org/10.1016/j.solener.2011.05.014.
[34] T. Kawanami, K. Togashi, K. Fumoto, S. Hirano, P. Zhang, K. Shirai, S. Hirasawa, Thermophysical properties and thermal characteristics of phase change emulsion for thermal energy storage media, Energy 117 (2016) 562–568, https://doi.org/10.1016/j.energy.2016.04.021.
[35] V. Mikkola, S. Puupponen, K. Saari, T. Ala-Nissila, A. Seppälä, Thermal properties and convective heat transfer of phase changing paraffin nanofluids, Int. J. Therm. Sci. 117 (2017) 163–171, https://doi.org/10.1016/j.ijthermalsci.2017.03.024.
[36] I. Ryklin, B. Byers, 26 - shear-thinning lamellar gel network emulsions as delivery systems, in: M.R. Rosen (Ed.), Deliv. Syst. Handb. Pers. Care Cosmet. Prod., William Andrew Publishing, Norwich, NY, 2005, pp. 547–568, https://doi.org/10.1016/B978-081551504-3.50031-6.
[37] B.P. Binks, Modern Aspects of Emulsion Science, Royal Society of Chemistry, Information Services, Cambridge, UK, 1998.
[38] A. Al-Ahmed, A. Sarı, M.A.J. Mazumder, B. Salhi, G. Hekimoğlu, F.A. Al-Sulaiman, Inamuddin, Thermal energy storage and thermal conductivity properties of fatty acid/fatty acid-grafted-CNTs and fatty acid/CNTs as novel composite phase change materials, Sci. Rep. 10 (2020), 15388, https://doi.org/10.1038/s41598-020-71891-1.
[39] P. Chatterjee, G.A. Sowiak, P.T. Underhill, Effect of phase change on the rheology and stability of paraffin wax-in-water Pickering emulsions, Rheol. Acta 56 (2017) 601–613, https://doi.org/10.1007/s00397-017-1021-4.
[40] S.A. Vanapalli, J.N. Coupland, Emulsions under shear—the formation and properties of partially coalesced lipid structures, Food Hydrocolloids 15 (2001) 507–512, https://doi.org/10.1016/S0268-005X(01)00057-1.
[41] S. Yoo, E. Kandare, R. Shanks, A.A. Khatibi, Viscoelastic characterization of multifunctional composites incorporated with microencapsulated phase change

materials, Mater. Today Proc. 4 (2017) 5239–5247, https://doi.org/10.1016/j.matpr.2017.05.033.
[42] C. Liu, Z. Zheng, C. Xi, Y. Liu, Exploration of the natural waxes-tuned crystallization behavior, droplet shape and rheology properties of O/W emulsions, J. Colloid Interface Sci. 587 (2021) 417–428, https://doi.org/10.1016/j.jcis.2020.12.024.
[43] N.V. Pogodina, S.K. Siddiquee, J.W. van Egmond, H.H. Winter, Correlation of rheology and light scattering in isotactic polypropylene during early stages of crystallization, Macromolecules 32 (1999) 1167–1174, https://doi.org/10.1021/ma980737x.
[44] N.V. Pogodina, V.P. Lavrenko, S. Srinivas, H.H. Winter, Rheology and structure of isotactic polypropylene near the gel point: quiescent and shear-induced crystallization, Polymer 42 (2001) 9031–9043, https://doi.org/10.1016/S0032-3861(01)00402-5.
[45] Y. Bin, L. Ma, R. Adachi, H. Kurosu, M. Matsuo, Ultra-drawing of low molecular weight polyethylene — ultra-high molecular weight polyethylene blend films prepared by gelation/crystallization from semi-dilute solutions, Polymer 42 (2001) 8125–8135, https://doi.org/10.1016/S0032-3861(01)00302-0.
[46] L. Gentile, C. Oliviero Rossi, U. Olsson, Rheological and rheo-SALS investigation of the multi-lamellar vesicle formation in the C12E3/D2O system, J. Colloid Interface Sci. 367 (2012) 537–539, https://doi.org/10.1016/j.jcis.2011.10.057.
[47] R. Pal, Effect of droplet size on the rheology of emulsions, AIChE J. 42 (1996) 3181–3190, https://doi.org/10.1002/aic.690421119.
[48] B.C. Tatar, G. Sumnu, S. Sahin, Chapter 17 - rheology of emulsions, in: J. Ahmed, P. Ptaszek, S. Basu (Eds.), Adv. Food Rheol. Its Appl., Woodhead Publishing, 2017, pp. 437–457, https://doi.org/10.1016/B978-0-08-100431-9.00017-6.
[49] R. Pal, Shear viscosity behavior of emulsions of two immiscible liquids, J. Colloid Interface Sci. 225 (2000) 359–366, https://doi.org/10.1006/jcis.2000.6776.
[50] L.L. Schramm, Emulsions, Foams, and Suspensions: Fundamentals and Applications, John Wiley & Sons, 2006.
[51] F. Mustan, N. Politova-Brinkova, Z. Vinarov, D. Rossetti, P. Rayment, S. Tcholakova, Interplay between bulk aggregates, surface properties and foam stability of nonionic surfactants, Adv. Colloid Interface Sci. 302 (2022), 102618, https://doi.org/10.1016/j.cis.2022.102618.
[52] J.F. Steffe, Rheological Methods in Food Process Engineering, Freeman Press, 1996.
[53] M.A. Delgado, J.M. Franco, P. Partal, C. Gallegos, Experimental study of grease flow in pipelines: wall slip and air entrainment effects, Chem. Eng. Process. Process Intensif. 44 (2005) 805–817, https://doi.org/10.1016/j.cep.2004.09.003.
[54] H. Fukushima, Y. Ogino, G. Matsuba, K. Nishida, T. Kanaya, Crystallization of polyethylene under shear flow as studied by time resolved depolarized light scattering. Effects of shear rate and shear strain, Polymer 46 (2005) 1878–1885, https://doi.org/10.1016/j.polymer.2004.12.048.
[55] T. Morimoto, H. Kumano, Flow and heat transfer characteristics of phase change emulsions in a circular tube: Part 1. Laminar flow, Int. J. Heat Mass Tran. 117 (2018) 887–895, https://doi.org/10.1016/j.ijheatmasstransfer.2017.10.055.
[56] J. Shao, J. Darkwa, G. Kokogiannakis, Development of a novel phase change material emulsion for cooling systems, Renew. Energy 87 (2016) 509–516, https://doi.org/10.1016/j.renene.2015.10.050.
[57] K. Almdal, J. Dyre, S. Hvidt, O. Kramer, Towards a phenomenological definition of the term 'gel, Polym. Gels Netw. 1 (1993) 5–17, https://doi.org/10.1016/0966-7822(93)90020-I.
[58] C. Liu, J. He, E. van Ruymbeke, R. Keunings, C. Bailly, Evaluation of different methods for the determination of the plateau modulus and the entanglement molecular weight, Polymer 47 (2006) 4461–4479, https://doi.org/10.1016/j.polymer.2006.04.054.
[59] S. Li, Q. Huang, L. Wang, K. Fan, Research on viscoelastic properties of water in waxy crude oil emulsion gels with the effect of droplet size and distribution, Can. J. Chem. Eng. 93 (2015) 2233–2244, https://doi.org/10.1002/cjce.22324.
[60] G. Li, W.J. Lee, N. Liu, X. Lu, C.P. Tan, O.M. Lai, C. Qiu, Y. Wang, Stabilization mechanism of water-in-oil emulsions by medium- and long-chain diacylglycerol: post-crystallization vs. pre-crystallization, Lebensm. Wiss. Technol. 146 (2021), 111649, https://doi.org/10.1016/j.lwt.2021.111649.
[61] J. Li, J. Cao, Q. Ren, Y. Ding, H. Zhu, C. Xiong, R. Chen, Effect of nano-silica and silicone oil paraffin emulsion composite waterproofing agent on the water resistance of flue gas desulfurization gypsum, Construct. Build. Mater. 287 (2021), 123055, https://doi.org/10.1016/j.conbuildmat.2021.123055.
[62] N. Gaudino, S.M. Ghazani, S. Clark, A.G. Marangoni, N.C. Acevedo, Development of lecithin and stearic acid based oleogels and oleogel emulsions for edible semisolid applications, Food Res. Int. 116 (2019) 79–89, https://doi.org/10.1016/j.foodres.2018.12.021.
[63] J.N. Coupland, Crystallization in emulsions, Curr. Opin. Colloid Interface Sci. 7 (2002) 445–450, https://doi.org/10.1016/S1359-0294(02)00080-8.
[64] N. Denkov, D. Cholakova, S. Tcholakova, S.K. Smoukov, On the mechanism of drop self-shaping in cooled emulsions, Langmuir 32 (2016) 7985–7991, https://doi.org/10.1021/acs.langmuir.6b01626.
[65] S. Guttman, Z. Sapir, M. Schultz, A.V. Butenko, B.M. Ocko, M. Deutsch, E. Sloutskin, How faceted liquid droplets grow tails, Proc. Natl. Acad. Sci. USA 113 (2016) 493–496, https://doi.org/10.1073/pnas.1515614113.
[66] D. Kashchiev, N. Kaneko, K. Sato, Kinetics of crystallization in polydisperse emulsions, J. Colloid Interface Sci. 208 (1998) 167–177, https://doi.org/10.1006/jcis.1998.5760.